Supplementary Information

Protein fold determined by paramagnetic magic-angle spinning solid-state NMR spectroscopy

Ishita Sengupta[1], Philippe S. Nadaud[1], Jonathan J. Helmus[1],
Charles D. Schwieters[2] and Christopher P. Jaroniec[1]*

[1]Department of Chemistry, The Ohio State University, 100 West 18th Avenue,
Columbus, Ohio 43210, USA
[2]Division of Computational Bioscience, Center for Information Technology, Building 12A,
National Institutes of Health, Bethesda, Maryland 20892, USA

*E-mail: jaroniec@chemistry.ohio-state.edu

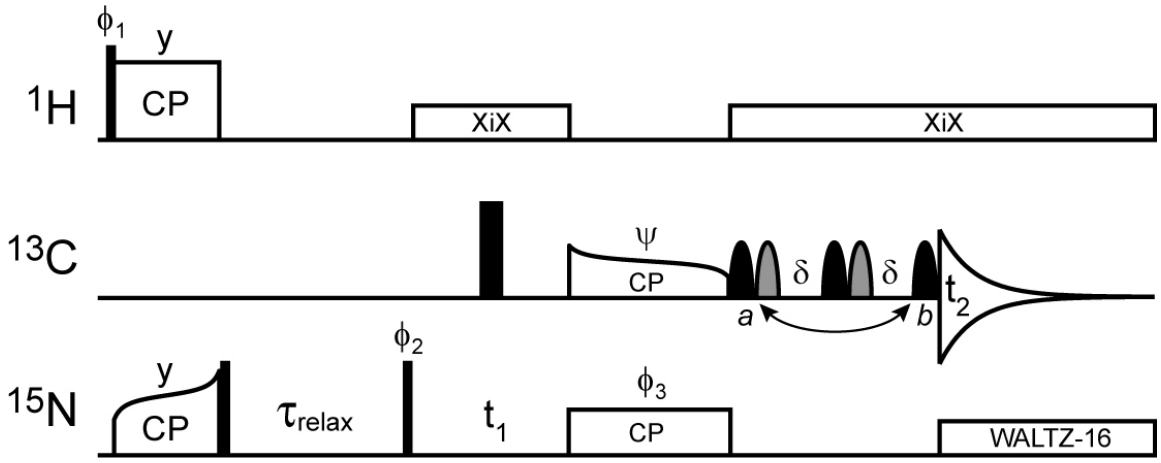

Figure S1. The pulse scheme used to determine residue-specific longitudinal ^{15}N relaxation rate constants, R_1, in the GB1 Cys-EDTA-Cu^{2+}/Zn^{2+} mutants from series of two-dimensional ^{15}N-^{13}CO (2D NCO) correlation spectra recorded with different values of τ_{relax} in the 100 μs to 4 s range.[1] The experiments were performed at 11.7 T (500 MHz ^{1}H Larmor frequency) and 40 kHz MAS rate. Narrow and wide black rectangles correspond to 90^o and 180^o pulses, respectively, and all pulses have phase *x* unless indicated otherwise. The ^{1}H, ^{13}C and ^{15}N carriers were placed at ~4.7, 175, and 120 ppm, respectively. ^{1}H-^{15}N cross-polarization (CP)[2] was achieved with a ~60 kHz ^{15}N field applied with a tangent ramp,[3] a ~100 kHz ^{1}H field, and a contact time of 1.0 ms. SPECIFIC CP[4] with a ~15 kHz ^{15}N field, a ~25 kHz ^{13}C field with a tangent ramp, and a 7 ms contact time was used to establish the ^{15}N-^{13}CO magnetization transfer. Proton XiX[5] and nitrogen WALTZ-16[6] decoupling was applied at field strengths of ~12 kHz and ~3.3 kHz, respectively, during periods indicated in the figure. The spin-state-selective excitation (S^{3}E) ^{13}CO-^{13}Cα J-decoupling scheme,[7,8] with the delay δ = 2.25 ms, consisted of two separate spectra recorded with selective rSNOB 180^o refocusing pulses[9] of 250 μs duration applied to the ^{13}CO spins at the frequency of 175 ppm (filled black shapes) and ^{13}Cα spins at the frequency of 55 ppm (filled gray shapes) in either position *a* or *b*. The spectra were processed as described by Laage et al.[8] The following phase cycles were employed to record spectra *a* and *b*. Spectrum *a*: φ_1 = 2(*x*), 2(-*x*); φ_2 = *x*, -*x*; φ_3 = *y*; ψ = *x*; *receiver* = *x*, -*x*, -*x*, *x*. Spectrum *b*: φ_1 = 2(*x*), 2(-*x*); φ_2 = *x*, -*x*; φ_3 = *y*; ψ = -*y*; *receiver* = *x*, -*x*, -*x*, *x*. Quadrature in the ^{15}N dimension was achieved by alternating phase φ_2 according to the States method.[10]

Table S1. Summary of longitudinal amide ^{15}N PRE restraints and repulsive 'NOE-type' distance restraints determined for the six GB1 mutants modified with paramagnetic EDTA-Cu^{2+} tags

EDTA-Cu^{2+} tag position	Residue number	PRE, Γ_1^N (s^{-1})[a]	Residue number	NOE[b]
8	4	0.14 ± 0.01	2	*
	5	0.26 ± 0.02	17	*
	9	0.34 ± 0.05	18	*
	14	0.52 ± 0.05	19	*
	15	0.54 ± 0.11	20	*
	39	0.15 ± 0.01	21	*
	40	0.24 ± 0.03	24	*
	41	0.14 ± 0.03	25	*
	43	0.27 ± 0.02	26	*
	44	0.22 ± 0.03	27	*
	45	0.14 ± 0.01	28	*
	46	0.14 ± 0.01	29	*
	47	0.11 ± 0.01	30	*
	50	0.11 ± 0.02	31	*
	51	0.14 ± 0.01	32	*
	52	0.18 ± 0.01	33	*
	53	0.29 ± 0.02	34	*
	55	0.54 ± 0.11	35	*
	56	0.20 ± 0.05	36	*
			37	*
			38	*
			48	*
			49	*
19	5	0.19 ± 0.02	7	*
	9	0.18 ± 0.01	14	*
	10	0.24 ± 0.04	33	*
	11	0.19 ± 0.02	34	*
	12	0.12 ± 0.02	35	*
	15	0.14 ± 0.01	37	*
	16	0.21 ± 0.01	43	*
	20	0.74 ± 0.09	45	*
	21	0.11 ± 0.01	46	*
	23	0.19 ± 0.03	53	*
	25	0.11 ± 0.02	54	*
	26	0.17 ± 0.01		
	28	0.14 ± 0.01		
	38	0.12 ± 0.01		
	39	0.13 ± 0.02		
	40	0.22 ± 0.03		
	41	0.18 ± 0.04		
	42	0.22 ± 0.03		
	47	0.12 ± 0.01		

Table S1. continued

EDTA-Cu^{2+} tag position	Residue number	PRE, Γ_1^N (s^{-1})[a]	Residue number	NOE[b]
	49	0.12 ± 0.01		
	51	0.15 ± 0.01		
	55	0.15 ± 0.02		
28	21	0.13 ± 0.01	2	*
	24	0.33 ± 0.02	4	*
	25	0.81 ± 0.05	5	*
	26	0.21 ± 0.01	6	*
	27	0.21 ± 0.01	7	*
	28	0.56 ± 0.07	8	*
	29	0.48 ± 0.03	9	*
	30	0.22 ± 0.01	10	*
	31	0.34 ± 0.03	11	*
	32	0.51 ± 0.02	12	*
	33	0.18 ± 0.01	13	*
	34	0.13 ± 0.01	14	*
	35	0.19 ± 0.01	15	*
	36	0.12 ± 0.01	17	*
	40	0.16 ± 0.01	18	*
	41	0.23 ± 0.02	19	*
	42	0.14 ± 0.01	20	*
	43	0.17 ± 0.01	37	*
			38	*
			39	*
			44	*
			45	*
			46	*
			47	*
			48	*
			49	*
			50	*
			51	*
			52	*
			53	*
			54	*
			55	*
			56	*
42	9	0.20 ± 0.01	7	*
	10	0.33 ± 0.09	14	*
	11	0.25 ± 0.06	18	*
	15	0.12 ± 0.01	19	*
	32	0.21 ± 0.03	20	*
	33	0.15 ± 0.01	21	*
	34	0.24 ± 0.03	24	*

Table S1. continued

EDTA-Cu^{2+} tag position	Residue number	PRE, Γ_1^N (s^{-1})[a]	Residue number	NOE[b]
	35	0.33 ± 0.03	25	*
	36	0.21 ± 0.01	26	*
	37	0.19 ± 0.01	27	*
	38	0.38 ± 0.02	29	*
	39	0.18 ± 0.02	30	*
	43	0.56 ± 0.03	45	*
	44	0.15 ± 0.01	47	*
	55	0.39 ± 0.02	48	*
	56	0.48 ± 0.13	49	*
			50	*
			51	*
			52	*
46	6	0.33 ± 0.03	9	*
	7	0.38 ± 0.03	10	*
	8	0.15 ± 0.03	11	*
	17	0.17 ± 0.02	13	*
	19	0.13 ± 0.03	14	*
	21	0.12 ± 0.01	15	*
	23	0.18 ± 0.02	18	*
	24	0.16 ± 0.01	29	*
	25	0.12 ± 0.02	30	*
	32	0.11 ± 0.02	31	*
	33	0.11 ± 0.02	40	*
	34	0.12 ± 0.03	42	*
	35	0.15 ± 0.03	55	*
	36	0.14 ± 0.03		
	37	0.12 ± 0.02		
	38	0.13 ± 0.03		
	39	0.12 ± 0.02		
	41	0.25 ± 0.02		
	43	0.11 ± 0.02		
	44	0.21 ± 0.03		
	45	0.36 ± 0.02		
	51	1.11 ± 0.15		
	52	0.37 ± 0.04		
	56	0.13 ± 0.01		
53	2	0.15 ± 0.02	9	*
	5	0.15 ± 0.01	10	*
	6	0.13 ± 0.02	11	*
	7	0.18 ± 0.05	13	*
	12	0.14 ± 0.03	16	*
	14	0.14 ± 0.03	17	*
	15	0.15 ± 0.03	19	*

Table S1. continued

EDTA-Cu^{2+} tag position	Residue number	PRE, Γ_1^N (s^{-1})[a]	Residue number	NOE[b]
	21	0.12 ± 0.01	24	*
	43	0.12 ± 0.01	25	*
	49	0.17 ± 0.04	27	*
	51	0.21 ± 0.03	29	*
			31	*
			32	*
			33	*
			34	*
			36	*
			37	*
			38	*
			39	*
			41	*
			42	*
			46	*

[a]PREs were calculated as $\Gamma_1^N = R_1(Cu^{2+}) - R_1(Zn^{2+})$, where ^{15}N R_1 values for the corresponding pair of EDTA-Cu^{2+} and EDTA-Zn^{2+} tagged proteins were obtained by fitting residue-specific relaxation trajectories to decaying single exponentials. A total of 110 quantitative PRE restraints (77 for residues located in regular secondary structure elements and 33 for loop residues) were determined for the six GB1 analogs and used in the structure calculations via the PREPot potential term (see main text and Supplementary Table S3 for additional details).

[b]For residues where the PRE measurements yielded values of $\Gamma_1^N \leq 0.10$ s^{-1} (indicated by asterisks) the PRE restraints were converted into purely repulsive 'NOE-type' distance restraints with a lower-bound cutoff of 15.1 Å and used in the structure calculations via the NOEPot potential term. A total of 121 residues for the six GB1 analogs fell into this category (89 located in regular secondary structure elements and 32 loop residues).

Table S2. TALOS+ dihedral angle restraints for GB1[a]

Residue number	ϕ (degrees)	ψ (degrees)
2	-115 ± 36	140 ± 36
3	-129 ± 26	149 ± 22
4	-133 ± 22	132 ± 20
5	-110 ± 24	122 ± 20
6	-105 ± 30	117 ± 30
7	-101 ± 30	124 ± 30
8	-108 ± 54	135 ± 54
9	-109 ± 70	170 ± 40
10	-67 ± 30	-32 ± 22
11	-102 ± 34	-4 ± 32
12	-117 ± 62	128 ± 42
13	-125 ± 28	161 ± 28
14	-150 ± 62	161 ± 34
15	-135 ± 34	151 ± 26
16	-121 ± 34	151 ± 32
17	-132 ± 20	156 ± 20
18	-128 ± 40	138 ± 26
19	-121 ± 20	129 ± 22
20	-114 ± 54	163 ± 30
21	-84 ± 36	-18 ± 32
22	–	–
23	-62 ± 20	-37 ± 20
24	-63 ± 20	-40 ± 20
25	-68 ± 20	-38 ± 20
26	-63 ± 20	-42 ± 20
27	-63 ± 20	-40 ± 24
28	-61 ± 20	-41 ± 20
29	-64 ± 20	-46 ± 20
30	-67 ± 20	-37 ± 20
31	-65 ± 20	-42 ± 20
32	-67 ± 20	-41 ± 20
33	-64 ± 20	-44 ± 20
34	-63 ± 20	-44 ± 20
35	-60 ± 20	-43 ± 20
36	-61 ± 20	-27 ± 20
37	-97 ± 26	7 ± 20
38	86 ± 20	13 ± 20
39	-84 ± 32	134 ± 20
40	-115 ± 48	138 ± 44
41	–	–
42	-113 ± 32	128 ± 36
43	-111 ± 38	151 ± 28
44	-129 ± 44	158 ± 22
45	-145 ± 32	134 ± 34

Table S2. continued

Residue number	ϕ (degrees)	ψ (degrees)
46	-112 ± 32	133 ± 32
47	–	–
48	-74 ± 22	-25 ± 38
49	-104 ± 20	6 ± 34
50	61 ± 22	34 ± 32
51	-102 ± 48	133 ± 20
52	-116 ± 26	153 ± 32
53	-129 ± 30	147 ± 20
54	-129 ± 26	132 ± 20
55	-107 ± 42	127 ± 28

[a]Dihedral restraints were obtained using the ^{13}C and ^{15}N solid-state NMR chemical shifts reported for microcrystalline GB1 (BMRB entry 15156) and the TALOS+ program[11] in the 'no-proton' mode (http://spin.niddk.nih.gov/bax/nmrserver/talos/). For predicted dihedral angles having uncertainties of less than $\pm 20^o$, the uncertainties were set to $\pm 20^o$ for the structure calculations.

Table S3. Potential term parameters during structure calculations

Potential name (force constant units)	Description	Force constant schedule[a]	
		Initial minimization and dynamics	Simulated annealing
PrePot (kcal·sec/mol)	SSNMR PRE restraints	0.05	ramped: 0.05 → 1.0
NOEPot (kcal/mol/Å^2)	repulsive distance restraints	2	ramped: 2 → 30
CDIH (kcal/mol/rad^2)	TALOS+ based dihedral restraints	1000	1000
COLL (kcal/mol/Å^2)	radius of gyration restraint	1000	1000
RAMA (kcal/mol)	knowledge-based dihedral restraints	1	1
HBDB (kcal/mol)	knowledge-based hydrogen bond restraints	2/1	2/1
ResidueAffPot (kcal/mol/Å)	knowledge-based contact potential	50/1	50/1
BOND (kcal/mol/Å^2)	bond length	1000	1000
ANGL (kcal/mol/rad^2)	bond angle	200	ramped: 200 → 500
IMPR (kcal/mol/rad^2)	improper dihedral angle	50	ramped: 50 → 5000
DIHE (kcal/mol/rad^2)[b]	dihedral angle	50	ramped: 50 → 5000
VDW (kcal/mol/Å^4)[c]	quartic atom-atom repulsion	0.004 Cα-only	ramped: 0.004 → 4 all atoms

[a]Entries with two slash-separated values correspond to the anneal value and refine value, respectively.
[b]Only applied to the EDTA-Cu^{2+} sidechain dihedral angles for which the **RAMA** term contains no information.
[c]In addition atomic radii are scaled by a value of 1.2 during initial dynamics and minimization and scaled by a value ramped from 0.9 to 0.78 during simulated annealing.

References

1. Nadaud, P. S., Helmus, J. J., Sengupta, I. & Jaroniec, C. P. Rapid acquisition of multidimensional solid-state NMR spectra of proteins facilitated by covalently bound paramagnetic tags. *J. Am. Chem. Soc.* **132**, 9561-9563 (2010).
2. Pines, A., Gibby, M. G. & Waugh, J. S. Proton-enhanced NMR of dilute spins in solids. *J. Chem. Phys.* **59**, 569-590 (1973).
3. Hediger, S., Meier, B. H. & Ernst, R. R. Adiabatic passage Hartmann-Hahn cross-polarization in NMR under magic-angle sample spinning. *Chem. Phys. Lett.* **240**, 449-456 (1995).
4. Baldus, M., Petkova, A. T., Herzfeld, J. & Griffin, R. G. Cross polarization in the tilted frame: assignment and spectral simplification in heteronuclear spin systems. *Mol. Phys.* **95**, 1197-1207 (1998).
5. Detken, A., Hardy, E. H., Ernst, M. & Meier, B. H. Simple and efficient decoupling in magic-angle spinning solid-state NMR: the XiX scheme. *Chem. Phys. Lett.* **356**, 298-304 (2002).
6. Shaka, A. J., Keeler, J. & Freeman, R. Evaluation of a new broadband decoupling sequence: WALTZ-16. *J. Magn. Reson.* **53**, 313-340 (1983).
7. Meissner, A., Duus, J. O. & Sorensen, O. W. Spin-state-selective excitation. Application for E.COSY-type measurement of J(HH) coupling constants. *J. Magn. Reson.* **128**, 92-97 (1997).
8. Laage, S. *et al.* Transverse-dephasing optimized homonuclear J-decoupling in solid-state NMR spectroscopy of uniformly ^{13}C-labeled proteins. *J. Am. Chem. Soc.* **131**, 10816-10817 (2009).
9. Kupce, E., Boyd, J. & Campbell, I. D. Short selective pulses for biochemical applications. *J. Magn. Reson. B* **106**, 300-303 (1995).
10. States, D. J., Haberkorn, R. A. & Ruben, D. J. A two-dimensional nuclear Overhauser experiment with pure absorption phase in four quadrants. *J. Magn. Reson.* **48**, 286-292 (1982).
11. Shen, Y., Delaglio, F., Cornilescu, G. & Bax, A. TALOS+: A hybrid method for predicting protein backbone torsion angles from NMR chemical shifts. *J. Biomol. NMR* **44**, 213-223 (2009).